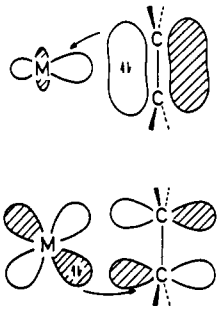

(2)

Upon reduction of TCNE, the C=C-centered π^*-acceptor orbital becomes singly occupied (LUMO → SOMO); thus, the effectiveness of d(metal)-to-π^*(olefin) back-bonding is diminished. On the other hand, the negative charge acquired on reduction turns $TCNE^{\bullet-}$ into an acceptable ligand of different character; the relatively long range of electrostatic interactions makes a coordination via the nitrile N lone pair more attractive. In fact, all known complexes in which TCNE is bound in the anion-radical oxidation state are either η^1-coordinated[2,3,8,11] or, in the case of coordinatively saturated metal components, form charge-transfer materials with noncoordinated $TCNE^{\bullet-}$.[15] Both positive shifts of the reduction potentials for the σ(N)-bonded isomers as well as the increased energetic splitting of carbonyl stretching frequencies of the coordinated $W(CO)_5$ after reduction are in agreement with diminished π-back-donation in this persistent secondary σ(N)-coordinated form.

Summarizing, we have presented an example for electron-transfer-induced isomerization which is distinguished both by a change of hapticity[6] of the metal *and* by a change of the type of donor atoms.[16,17] Although this isomerization represents a qualitatively significant structural change, it does not become apparent from cyclic voltammetric studies of the corresponding redox process at conventional scan rates. Extension of the potential range, variation of scan rates, and use of several spectroscopic methods proved to be necessary to detect and clarify the organometallic molecular hysteresis[6d] process (1).

Acknowledgment. This work was supported by grants from Deutsche Forschungsgemeinschaft, Volkswagenstiftung, and Fonds der Chemischen Industrie. We also thank Walter Matheis and Michael Moscherosch for their help with the HMO/McLachlan and EPR simulation programs.

(15) (a) Miller, J. S.; Epstein, A. J.; Reiff, W. M. *Acc. Chem. Res.* **1988**, *21*, 114. (b) Miller, J. S.; Calabrese, J. C.; Rommelmann, H.; Chittipeddi, S. R.; Zhang, J. H.; Reiff, W. M.; Epstein, A. J. *J. Am. Chem. Soc.* **1987**, *109*, 769.

(16) Cf.: Choi, M.-G.; Angelici, R. J. *J. Am. Chem. Soc.* **1991**, *113*, 5651.

(17) Electron-transfer-induced isomerization of a $W(CO)_5$ complex from N to Se coordination: (a) Kaim, W.; Kasack, V. *Angew. Chem.* **1982**, *94*, 712; *Angew. Chem., Int. Ed. Engl.* **1982**, *21*, 700. (b) Kaim, W. *J. Organomet. Chem.* **1984**, *264*, 317. (c) Kaim, W.; Kohlmann, S.; Lees, A. J.; Zulu, M. M. *Z. Anorg. Allg. Chem.* **1989**, *575*, 97.

Contribution from the Institute of Chemistry, University of Wrocław, 14 F. Joliot-Curie St., Wrocław, Poland

Nuclear Magnetic Resonance Study of the Molecular and Electronic Structure of Nickel(II) Tetraphenyl-21-thiaporphyrins†

Jerzy Lisowski, Lechosław Latos-Grażyński,* and Ludmiła Szterenberg

Received May 8, 1991

The proton NMR spectra of high-spin ($S = 1$) nickel(II) monohalide complexes of tetraphenyl-21-thiaporphyrin have been recorded and assigned by means of specific deuteration, methyl substitution, and line width consideration. The characteristic pattern of pyrrole (downfield) and thiophene resonances (upfield) has been established. The specific assignment of pyrrole resonances has been achieved by NOE measurements. Replacement of chloride by perchlorate results in formation of low-spin diamagnetic complex $Ni^{II}(STPP)ClO_4$ in chloroform. Imidazole replaces the axial halide ligand to produce five-coordinate derivatives that give resonances for the coordinated axial ligand. The formation of the six-coordinate form has been also established. It is apparent from the ^1H NMR studies of $Ni^{II}(STPP)Cl$ and related systems that the 21-thiaporphyrin macrocycle is flexible in solution. The structure of the equatorial macrocycle adjusts to the spin and electronic state of the $Ni^{II}(STPP)$ moiety, as determined by the nature and number of axial ligands. The pyrrole shift pattern has been related to the Ni(II) coordination number. The isotropic shifts of pyrroles and thiophene resonances are dominated by the σ-contact mechanism. The direct σ–π spin density transfer has been proposed to explain the upfield shift of the thiophene and a large difference in contact shifts of pyrrole resonances even for protons located in the same pyrrole ring. To account for the sulfur contribution and the geometry of 21-thiaporphyrin, the semiquantitative Fenske–Hall LCAO MO method has been used to determine molecular orbitals involved in the distribution of spin density via π-orbitals.

Introduction

Although porphyrins and related pyrrole compounds are among the most widely studied of all known macrocycles,[1] relatively little effort has been devoted to the development of macrocyclic systems where modification of porphyrin has been achieved by introduction of other donors (O, S, Se, NCH_3, NO, N–C) to replace one or more pyrrole nitrogens.[2-5] These new macrocycles are of interest as potential complexing agents. Limited reports on the oxaporphyrins, dithiaporphyrins, and diselenaporphyrins have appeared.[6] The tetraoxaporphyrin dication has recently been

* To whom correspondence should be addressed.

† Abbreviations: STPP, 5,10,15,20-tetraphenyl-21-thiaporphyrin anion; STTP, 5,10,15,20-tetrakis(*p*-tolyl)-21-thiaporphyrin anion; STPP-d_{10}, 5,20-diphenyl-10,15-bis(phenyl-d_5)-21-thiaporphyrin anion; STPP-d_6, 5,10,15,20-tetraphenyl-21-thiaporphyrin anion deuterated at pyrrole β-positions.

(1) Morgan, B.; Dolphin, D. *Struct. Bonding* **1987**, *64*, 115.

(2) (a) Lavallee, D. K. *The Chemistry and Biochemistry of N-substituted Porphyrins*; VCH Publisher Inc.: New York, 1987. (b) Saito, S.; Hano, H. A. *Proc. Natl. Acad. Sci. U.S.A.* **1981**, *78*, 5508. (c) Augusto, G.; Kunze, K. L.; Ortiz de Montellano, P. R. *J. Biol. Chem.* **1982**, *257*, 6231. (d) Lanceon, D. Cocolios, P.; Guillard, R.; Kadish, K. M. *J. Am. Chem. Soc.* **1984**, *106*, 4472. (e) Balch, A. L.; Renner, M. W. *J. Am. Chem. Soc.* **1986**, *108*, 2603. (f) Wysłouch, A.; Latos-Grażyński, L.; Grzeszczuk, M.; Drabent, K.; Bartczak, T. *J. Chem. Soc., Chem. Commun.* **1988**, 1377.

(3) (a) Balch, A. L.; Chan, Y.-W.; Olmstead, M. M.; Renner, M. W. *J. Am. Chem. Soc.* **1985**, *107*, 2393. (b) Balch, A. L.; Chan, Y.-W.; Olmstead, M. M. *J. Am. Chem. Soc.* **1985**, *107*, 6510. (c) Groves, J. T.; Watanabe, Y. *J. Am. Chem. Soc.* **1986**, *108*, 7836.

0020-1669/92/1331-1933$03.00/0

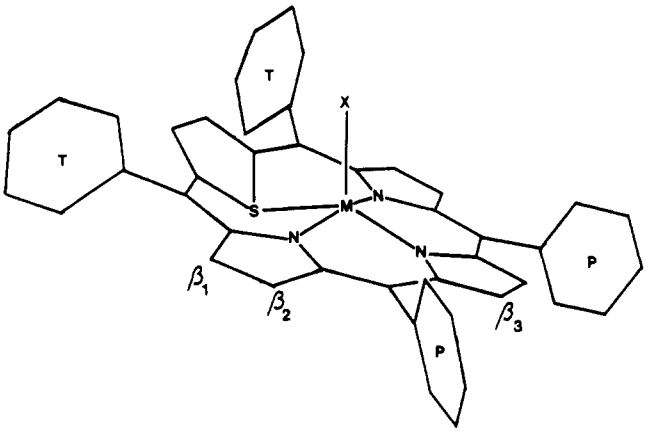

Figure 1. Drawing of the solid-state structure of Ni^{II}(STPP)Cl adapted from the X-ray crystallographic study. β positions and phenyl rings labeled with p and t subscripts are indicated.

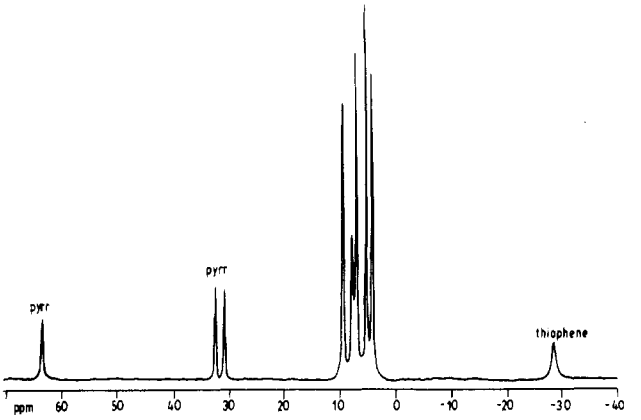

Figure 2. ^{1}H NMR spectrum of chloroform-*d* solutions at 298 K of Ni^{II}(STPP)Cl.

synthesized and discussed in the context of the aromatic character of annulenes.[7] In addition, the sulfur-containing system offers unique possibilities to explore coordinating properties of thiophene. Recently, we have reported the synthesis and characterization of a new macrocyclic ligand, 5,10,15,20-tetraphenyl-21-thiaporphyrin (STPPH), in which one of the pyrrole moieties is replaced by thiophene.[8]

This ligand coordinates a large variety of metal ions to form four-, five- and six-coordinate complexes[8-11] in which the thiophene fragment is bent out of the plane of the macrocycle. This bending opens up the center to accommodate the metal ion and allows it to bind the thiophene sulfur. Thus, the thiophene is η^1-bonded to the metal through a pyramidal sulfur atom. The flexibility of the thiaporphyrin allows it to accommodate metal ions of different ionic sizes including Ni(II) and Ni(I). The Ni(II)/Ni(I) couple is of special interest in understanding how changes in the macrocycle structure can lead to changes of the site of one-electron reduction of nickel(II) porphyrins, nickel(II) chlorins, nickel(II) bacteriochlorin, and nickel(II) porphycene.[12-14] Nickel(II) porphyrins and related compounds have been widely studied because of the growing interest in nickel(II) hydrocorphinoid derivatives, i.e. factor F_{430} which was identified as the active site of the methyl coenzyme M methyl reductase (from *Methanobacterium thermoautotrophicum*).[15-17] We have demonstrated

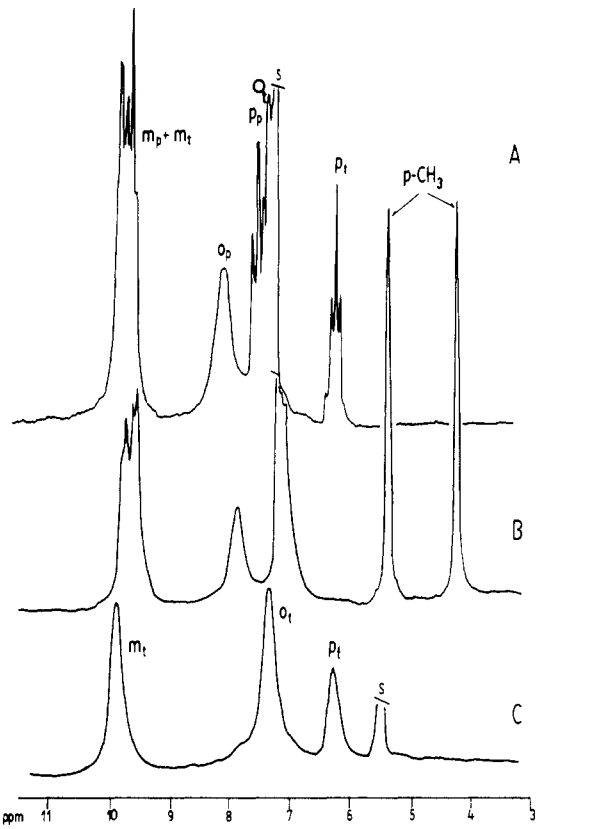

Figure 3. ^{1}H NMR spectra at 298 K in the +20 to −5 ppm region of (A) Ni^{II}(STPP)Cl in $CDCl_3$, (B) Ni^{II}(STTP)Cl in $CDCl_3$, and (C) Ni^{II}(STPP-d_{10})Cl in CD_2Cl_2. Peak labels are as in Figure 1.

the reduction of nickel(II) thiaporphyrin (Ni^{II}(STPP)Cl) to form stable nickel(I) thiaporphyrin (Ni^{I}(STPP)) and probed its coordination geometry.[18] In this paper we extend our studies to the ^{1}H NMR spectra of Ni^{II}(STPP)Cl and related complexes. Since Ni^{II}(STPP)Cl is paramagnetic there is the possibility of establishing a general relation between the isotropic shift pattern

(4) (a) Callot, H. J.; Chevrier, B.; Weiss, R. *J. Am. Chem. Soc.* **1978**, *100*, 1324. (b) Mansuy, D.; Morgenstern-Badrau, I.; Lange, M.; Gans, P. *Inorg. Chem.* **1982**, *21*, 1427. (c) Balch, A. L.; Cheng, R.-J.; La Mar, G. N.; Latos-Grażyński, L. *Inorg. Chem.* **1985**, *24*, 2651.
(5) (a) Broadhurst, M. J.; Grigg, R.; Johnson, A. W. *J. Chem. Soc. C* **1971**, 3681. (b) Johnson, A. W. In *Porphyrins and Metalloporphyrins*; Smith, K. M., Ed.; Elsevier: Amsterdam, 1975; p 279.
(6) (a) Ulman, A.; Manassen, J. *J. Am. Chem. Soc.* **1975**, *97*, 6540. (b) Ulman, A.; Manassen, J.; Frolow, F.; Rabinovich, D. *Tetrahedron Lett.* **1978**, 1855. (c) Ulman, A.; Manassen, J. *J. Chem. Soc., Perkin Trans. 1* **1979**, 1066. (d) Ulman, A.; Manassen, J.; Frolow, F.; Rabinovich, D. *Inorg. Chem.* **1981**, *20*, 1987. (e) Abraham, R. J.; Leonard, P.; Ulman, A. *Org. Magn. Reson.* **1984**, *22*, 561.
(7) (a) Vogel, E.; Haas, W.; Krupp, B.; Lex, J.; Schmickler, H. *Angew. Chem. Int., Ed. Engl.* **1988**, *27*, 406. (b) Vogel, E.; Röhring, P.; Sicken, M.; Knipp, B.; Herrman, A.; Pohl, M.; Schmickler, H.; Lex, J. *Angew. Chem., Int. Ed. Engl.* **1989**, *28*, 1651.
(8) Latos-Grażyński, L.; Lisowski, J.; Olmstead, M. M.; Balch, A. L. *J. Am. Chem. Soc.* **1987**, *109*, 4428.
(9) Latos-Grażyński, L.; Lisowski, J.; Olmstead, M. M.; Balch, A. L. *Inorg. Chem.* **1989**, *28*, 1183.
(10) Latos-Grażyński, L.; Lisowski, J.; Olmstead, M. M.; Balch, A. L. *Inorg. Chem.* **1989**, *28*, 3328.
(11) Latos-Grażyński, L.; Olmstead, M. M.; Balch, A. L. *Inorg. Chem.* **1989**, *28*, 4065.
(12) (a) Stolzenberg, A. M.; Stershic, M. T. *Inorg. Chem.* **1987**, *26*, 3082. (b) Stolzenberg, A. M.; Stershic, M. T. *J. Am. Chem. Soc.* **1988**, *110*, 5397. (c) Stolzenberg, A. M.; Stershic, M. T. *J. Am. Chem. Soc.* **1988**, *110*, 6391.
(13) Lexa, D.; Momenteau, M.; Mispelter, J.; Saveant, J. M. *Inorg. Chem.* **1989**, *28*, 30.
(14) Renner, M. W.; Forman, A.; Wu, W.; Chang, C. K.; Fajer, J. *J. Am. Chem. Soc.* **1989**, *111*, 8618.
(15) Ellefson, W. L.; Whitman, W. B.; Wolfe, R. S. *Proc. Natl. Acad. Sci. U.S.A.* **1982**, *79*, 3707.
(16) (a) Pfalz, A.; Jaun, B.; Fassler, A.; Eschenmoser, A.; Jaenchen, R.; Gilles, H. H.; Diekert, G.; Thauer, R. R. *Helv. Chim. Acta* **1982**, *65*, 828. (b) Livingston, D. A.; Pfaltz, A.; Schreiber, J.; Eschenmoser, A.; Ankel-Fusch, D.; Moll, J.; Jaenchen, R.; Thauer, R. K. *Helv. Chim. Acta* **1984**, *67*, 334. (c) Pfaltz, A.; Livingston, D. A.; Jaun, B.; Diekert, G.; Thauer, R.; Eschenmoser, A. *Helv. Chim. Acta* **1985**, *68*, 1338. (d) Pfaltz, A. In *The Bioinorganic Chemistry of Nickel*; Lancaster, J. R., Jr., Ed.; VCH Publishers Inc.: New York, 1988; p 275.
(17) Albracht, S. P. J.; Ankel-Fusch, D.; Van der Zwaan, J. W.; Fontijn, R. D.; Thauer, R. K. *Biochim. Biophys. Acta* **1986**, *870*, 50.
(18) Chmielewski, P.; Grzeszczuk, M.; Latos-Grażyński, L.; Lisowski, J. *Inorg. Chem.* **1989**, *28*, 3546.

Table I. Chemical Shifts[a]

	pyrrole				phenyl				
	β_1	β_2	β_3	thiophene	ortho$_t$	ortho$_p$	meta	para$_t$	para$_p$
Ni(STPP)Cl[b]	64.58	32.51	30.91	−29.84	7.31	8.10	9.93 9.81 9.74	6.17 (5.65)	7.53 (4.25)
Ni(STPP)Br[b]	63.19	31.20	29.60	−29.39	6.95	7.79	9.72 9.65 9.58	6.08	7.34
Ni(STPP)I[b]	55.42	29.65	23.35	−23.97	6.85	7.58	9.34	6.29	7.30
Ni(STPP)Cl[c]	67.72	35.89	56.32	−23.41	9.16	7.08	8.18 9.68	8.41	(4.16)
Ni(STPP)Cl[d]	68.5	36.0	57.0	−22.0	9.42	7.57	8.40 9.92	8.57	7.57
Ni(STPP)Cl[e]	63.88	31.72	35.62	−26.74			9.57	6.33	
Ni(STPP)Cl[f]	64.5	32.2	42.0	−25.5			9.08	6.78	7.50

[a] ppm vs TMS, 298 K. [b] In chloroform. [c] In DMSO. [d] In methanol. [e] In chloroform after addition of *n*-butylamine (1:1 molar ratio). [f] In chloroform after addition of *n*-butylamine (1:4 molar ratio). In parenthesis shifts for the methyl groups of Ni(STTP)Cl.

of the pyrrole macrocycle and its electronic and molecular structure. This may be of potential use to studies on Ni(II) coordinated in the active site of proteins. Utility of NMR spectroscopy as a very sensitive probe of molecular and electronic structure of paramagnetic metalloproteins and their model systems is well established.[19]

In particular, the coordination of nitrogen bases to the axial position of Ni^{II}(STPP)Cl mono and bis adducts has been a point of interest since rapid exchange of ligands prevented NMR characterization of substituted imidazoles bound to nickel(II) porphyrins.[20,21]

Results

Characterization and Spectral Assignments for Halide Complexes. Our analysis of the spectra of the Ni(II) thiaporphyrin halide complexes is based on the geometric information available from the X-ray studies.[9-11] The schematic structure of Ni^{II}(STPP)Cl as determined by X-ray diffraction is shown in Figure 1. While the molecule has no symmetry in the solid state, it appears to have C_s symmetry in solution with the mirror plane passing through the nickel atom, the axial chloride ligand, and the thiophene sulfur. Accordingly, labels have been affixed to the three pyrrole positions and to the phenyl rings. The NMR data have been analyzed in the context of the effective C_s geometry. In this case there are three distinct pyrrole protons and one thiophene proton. Two ortho and meta positions on each phenyl ring will be distinguishable because of the perpendicular orientation of these rings with respect to the porphyrin plane and the restricted rotation about meso-carbon-to-phenyl bond.[19a] However, the folding of the core of the Ni^{II}(STPP)Cl molecule may produce lowering of an activation barrier of rotation.[4c,19a,22] This results in an average chemical shift for both ortho and meta positions of T and P phenyl rings respectively. The ^{1}H NMR spectrum of Ni^{II}(STPP)Cl is shown in Figures 2 and 3. The resonance assignments which are given above each peak have been made on the basis of relative intensities, line width analysis, methyl substitution and site-specific deuteration. In order to identify pyrrole and phenyl resonances, the ^{1}H NMR spectra of Ni^{II}(STPP-d_6)Cl (pyrrole deuterated) and Ni^{II}(STPP-d_{10})Cl (P-phenyl deuterated) have been obtained. The most characteristic feature, the upfield peak at −29.84 ppm, corresponds to the thiophene protons. There are three downfield-shifted pyrrole resonances. Additional resonances in Figure 2 come from phenyl protons. Two para proton resonances have been unambiguously identified, since these resonances are missing in the spectrum of the *p*-tolyl derivative, and two new methyl resonances are present. The remaining phenyl resonances in Figure 3 fall into two groups according to their line width. The two broader resonances are assigned to ortho protons since these should relax more efficiently because they are close to the paramagnetic Ni(II) ion.[19a] The remaining multiplet at 9.5 ppm has been assigned to the *m*-phenyl resonances. The para and meta resonances are coupled to one another. Trace A of Figure 3 shows the expected triplet character of para resonances due to spin–spin coupling to the two nearly equivalent meta protons. The pattern of meta resonances results from overlapping of two meta doublets. Figure 3 shows an expansion of the T and P phenyl region. Notice that a set of three resonances (o_p, m_p, p_p) is absent from the spectrum of Ni^{II}(STPP-d_{10})Cl (P-phenyl deuterated) (trace C). This resulted in the selective assignment of T- and P-phenyl protons. The two ortho and two meta protons on each ring may be inequivalent since the porphyrin plane bears different substituents on opposite sides. This inequivalence prevails if the rotation about the meso-carbon–phenyl bond is restricted. However the Ni^{II}(STPP)Cl spectrum corresponds to the situation where the rotation is relatively fast (298 K, $CDCl_3$, 100 MHz). The *m*- and *o*-phenyl resonances demonstrated signs of dynamic broadening at −60 °C.

Ortho methyl substitution of the T and P phenyls results in formation of eight atropisomers, a phenomenon previously seen for Ni(NCH$_3$TPP)Cl,[21] which has similar symmetry. Steric hindrance of the methyl group freezes rotation, and complex multiplet structure for the meta protons (10 resonances) could be observed. The presence of atropisomers results also in the multiplet structure of pyrrole and thiophene resonances.

Curie plots for pyrrole and thiophene resonances are shown in Figure 4. The data show the linear behavior with extrapolated intercepts that are fairly close to the diamagnetic positions observed for a suitable model, Pd^{II}(STPP)Cl.[23]

^{1}H NMR data are presented in Table I. Spectral assignments for Ni^{II}(STPP)Br and Ni^{II}(STPP)I have been made by analogy to Ni^{II}(STPP)Cl. Changes of axial anions in the series Cl$^-$, Br$^-$, I$^-$ results in the systematic decrease of the isotropic shifts, but the general spectral pattern is preserved. Solvent effects have been found. In chloroform, dichloromethane, benzene, and toluene small spectral changes are due to nonspecific solvent–porphyrin interactions. Drastically different spectra of Ni^{II}(STPP)Cl in dimethyl sulfoxide or methanol are attributed to solvent coordination with formation of [Ni^{II}(STPP)(solvent)$_2$]Cl. This stoichiometry is assumed on the basis of analogy with the imidazole bis adducts of Ni^{II}(STPP)Cl (vide infra).

Assignments by Nuclear Overhauser Effect. The NOE has been used to assign resonances in paramagnetic hemoproteins[24,25] and

(19) (a) La Mar, G. N.; Walker, F. A. In *Porphyrins*; Dolphin, D., Ed.; Academic Press: New York, 1979; Vol. IVB, p 61. (b) Bertini, I.; Luchinat, C. In *NMR of Paramagnetic Molecules in Biological Systems*; The Benjamin/Cumming Publishing Co. Inc.: Menlo Park, CA, 1986.
(20) Walker, F. A. In *Porphyrins*; Dolphin, D., Ed.; Academic Press: New York, 1979; Vol. IVB, p 129.
(21) Latos-Grażyński, L. *Inorg. Chem.* **1985**, *24*, 1681.
(22) Eaton, S. S.; Fishwild, D. M.; Eaton, G. R. *Inorg. Chem.* **1978**, *17*, 1542 and references cited therein.
(23) Latos-Grażyński, L.; Lisowski, J.; Balch, A. L. Unpublished results.
(24) Unger, S. W.; Lecomte, J. T. J.; La Mar, G. N. *J. Magn. Reson.* **1985**, *64*, 521.
(25) Emerson, S. D.; Lecomte, J. T. J.; La Mar, G. N. *J. Am. Chem. Soc.* **1988**, *110*, 4176.

Table II. Chemical[a] and Isotropic[b] Shifts of Coordinated (*R*)-Imidazoles

	[Ni(STPP)(Im)]Cl		[Ni(STPP)(2-MeIm)]Cl		[Ni(STPP)(5-MeIm)]Cl	
	chemical shift	isotropic shift	chemical shift	isotropic shift	chemical shift	isotropic shift
NH	74.48	61.78	75.57	62.87	76.64	63.94
2-H	57.58	56.53			58.33	57.53
4-H	53.50	53.00	52.32	53.02	54.86	54.46
5-H	52.72	48.32	40.23	36.03		
2-CH_3			-16.84	-14.28		
5-CH_3					-4.0	3.7

[a] In $CDCl_3$, 298 K, chemical shifts measured for the 1:0.5 Ni(STPP): (*R*)-imidazole molar ratio to avoid ligand-exchange effects. [b] Diamagnetic standards of coordinated imidazoles as in ref 45.

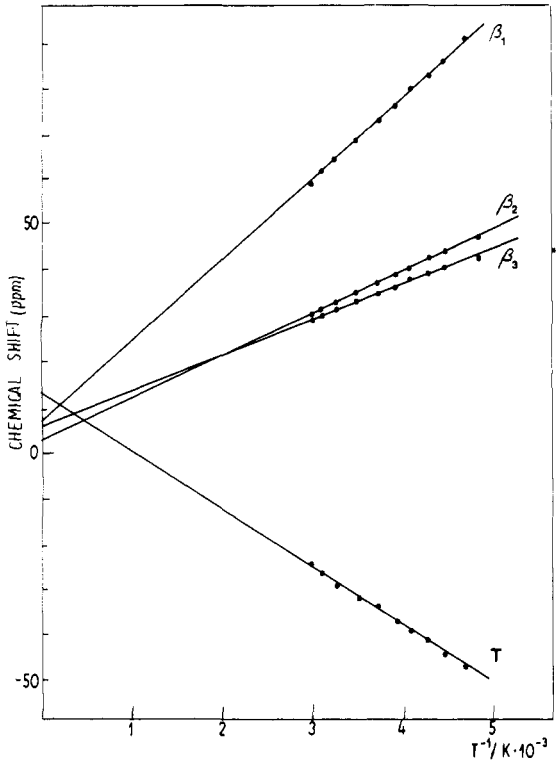

Figure 4. Curie plot of pyrrole (β) and thiophene (T) protons of Ni^{II}(STPP)Cl in chloroform-*d* solution.

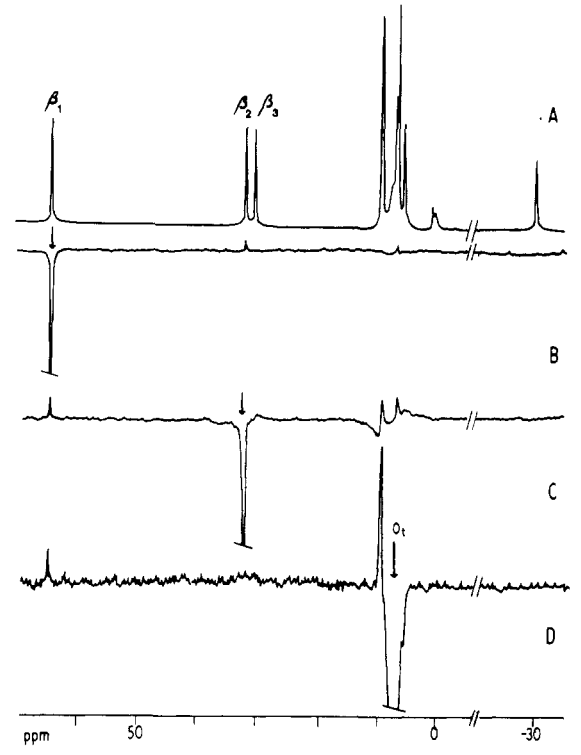

Figure 5. (A) 100-MHz reference spectrum of Ni^{II}(STPP)Cl in chloroform-*d* at 298 K. (B–D) Difference spectra generated by subtracting the reference spectrum from one in which the resonances indicated by arrows were presaturated. Assignments are as in Figure 1.

bovine superoxide dismutase[26] but has been less directly applicable to the model systems, i.e. metalloporphyrins. Models usually have reorientation times which place them in the intermediate motion region where ^1H–^1H NOEs are rather small, particularly at high magnetic fields. La Mar et al. demonstrated[27,28] that the molecular tumbling time is put in the slow motion limit if the molecules of interest are dissolved in viscous solvents. Under such condition, a large negative NOE could be readily observed for a monomeric complex of protoheme–bis(cyanide). In low-viscosity solvents, observable but positive NOEs are expected when the experiment is conducted at relatively low field.[27] In the case of Ni^{II}(STPP)Cl, the assignment of individual pyrrole resonances and those of the individual phenyls could be accomplished by NOE measurements at relatively low ^1H NMR frequency (100 MHz). The very narrow resonances of this complex facilitated these experiments. Figure 5 shows NOE difference spectra of Ni^{II}(STPP)Cl. The relevant spectrum taken with off-resonance irradiation is also presented. The observed NOEs were small (up to 3%) even for protons located on the same pyrrole ring. Irradiation of the pyrrole resonances at 64.58 ppm (298 K) yields weak positive NOEs at 32.51 ppm (pyrrole) and 7.31 ppm (trace B, Figure 5). The reciprocal NOE connectivities of the 64.58 ppm to the 32.51 and 7.31 ppm resonances are also shown in trace C of Figure 5. Irradiation of resonances at 30.91 ppm (pyrrole) and -29.84 ppm (thiophene) yield no detectable NOE. NOEs have been observed between ortho, meta, and para resonances of T- and P-phenyl rings. The pattern of connectivities is interpretable using the unambiguous assignment of the T-phenyl ortho proton resonance. The pyrrole resonance at 64.58 is readily assigned to the β_1 pyrrole proton (Figure 1) since it shows connectivity to the T phenyl ortho resonance (trace D, Figure 5). The pyrrole resonance at 32.51 ppm, which is connected to the β_1 pyrrole resonance, corresponds obviously to the β_2 pyrrole. The remaining pyrrole resonance (30.91 ppm) corresponds to the β_3 position.

Imidazole Coordination. Addition of imidazole and methyl-substituted imidazoles has been followed by ^1H NMR spectroscopy. Titration of a 5 mM solution of Ni^{II}(STPP)Cl with imidazole in $CDCl_3$ up to a 1:1 molar ratio shows the gradual growth of a new set of resonances while the resonances of the starting material diminish in intensity. The spectrum of the product is shown in trace A of Figure 6. All resonances of the coordinated imidazole are clearly discernible. Their integrated intensities indicate that only one imidazole ligand is bound in the first step of the reaction. Identical spectra have been obtained when Ni^{II}(STPP)Br or Ni^{II}(STPP)I has been used. This observation along with the fact that the overall pattern of the thiaporphyrin resonances and relative line widths appear to be retained in the spectrum of the imidazole adduct indicates that imidazole replaces

(26) Banci, L.; Bertini, I.; Luchinat, C.; Piccioli, M.; Scozzafava, A. *Inorg. Chem.* **1989**, *28*, 4650.
(27) Yu, C.; Unger, S. W.; La Mar, G. N. *J. Magn. Reson.* **1986**, *67*, 346.
(28) Liccocia, S.; Chatfield, M. J.; La Mar, G. N.; Smith, K. M.; Mansfield, K. E.; Anderson, R. C. *J. Am. Chem. Soc.* **1988**, *111*, 6087.

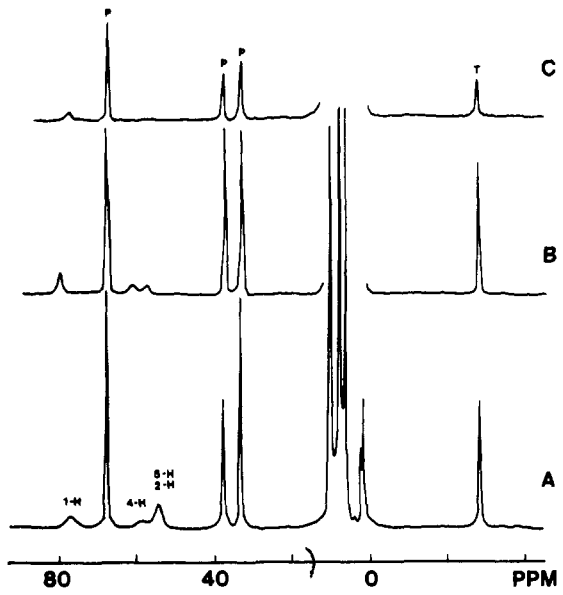

Figure 6. ^{1}H NMR spectra of 5 mM chloroform-*d* solutions of Ni^{II}(STPP)Cl in the presence of (A) imidazole, (B) 5-methylimidazole, (C) imidazole-d_3 (1:1 molar ratio, 298 K).

Table III. Chemical Shifts of [Ni(STPP)((*R*)-Im)$_n$]Cl Complexes[a]

compd	pyrrole[b] β_1	β_2	β_3	thiophene
[Ni(STPP)(Im)]Cl[c]	64.74	31.48	35.71	−26.89
[Ni(STPP)(1-MeIm)]Cl[d]	65.25	32.75	35.75	−28.55
[Ni(STPP)(2-MeIm)]Cl[c]	64.74	29.45	34.61	−24.34
[Ni(STPP)(5-MeIm)]Cl[c]	64.67	31.61	35.30	−27.16
[Ni(STPP)(Im)$_2$]Cl[e]	70.50	35.51	54.02	−24.75
[Ni(STPP)(1-MeIm)$_2$]Cl[e]	69.38	35.49	55.65	−24.47

[a] In chloroform, 298 K. [b] Labels as in Figure 1. [c] Chemical shifts measured for the 1:0.5 Ni(STPP)Cl:(*R*)-Im molar ratio. [d] Chemical shifts measured for the 1:1 Ni(STPP)Cl:1-MeIm molar ratio. [e] Chemical shifts measured for the 1:10 Ni(STPP)Cl:(*R*)-Im molar ratio.

the axial anion to form [Ni^{II}(STPP)(Im)]Cl. The imidazole resonances have been identified through suitable substitution(s). The data are summarized in Table II. The spectra obtained from 5-methylimidazole and imidazole-d_3 are shown in traces B and C of Figure 6. The resonance of 2-H is readily assigned since it is missing in the spectrum of [Ni^{II}(STPP)(imidazole-2-*d*)]Cl. All but the 1-NH imidazole resonances are missing in the spectrum of the imidazole-d_3 adduct (trace C, Figure 6). The 4-H resonance is assigned on the basis of its line width (140 Hz), which is similar to that of the 2-H resonance (150 Hz). Both are expected to be at similar distances from the nickel(II) ion, and both should have comparable widths that are greater than those of the other imidazole resonances (NH 97 Hz, 5-H 70 Hz). The 5-H resonance has been assigned to the peak at 52.72 ppm, since that peak is absent from the spectrum obtained for 4-methylimidazole (coordinates as its tautomeric form, 5-methylimidazole). There is a significant change in the spectral pattern of the 2-methylimidazole complex since the narrow 5-H resonance is shifted ca. 12 ppm upfield. This change is a consequence of the steric effect that arises from the introduction of the methyl group so close to the metal-binding site. The upfield shifted 2-CH_3 resonance is readily identified (Table II). At ratios of imidazole to Ni^{II}(STPP)Cl higher than 1.1:1 the coordinated imidazole resonances have not been detected as a result of exchange broadening. The smooth changes of the chemical shifts of the pyrrole and thiophene resonances have been observed begining with the 1.1:1 molar ratio to achieve asymptotic values for the 10:1 molar ratio (Table III). Under these conditions this must be the six-coordinated compound [Ni^{II}(STPP)(Im)$_2$]Cl which determinates the asymptotic chemical shift. Similar behavior has been established for 2-methylimidazole and 4-methylimidazole systems.

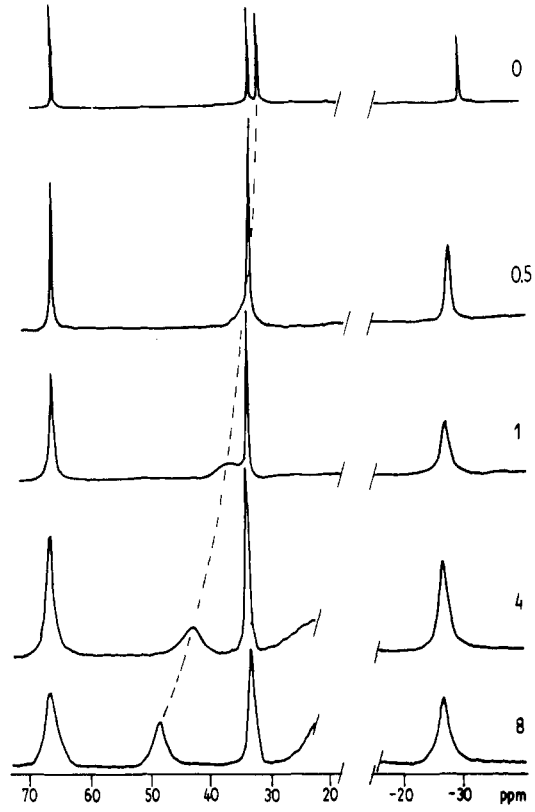

Figure 7. ^{1}H NMR titration of Ni^{II}(STPP)Cl with 1-methylimidazole (chloroform-*d*, 298 K). Number of 1-MeIm equivalents added is shown in the figure.

The titration of Ni^{II}(STPP)Cl with 1-methylimidazole exhibits a smooth shift change through the complete concentration range, as shown in Figure 7. The axial ligand lability precludes observation of the coordinated ligand peaks. The selective broadening of the thiophene and one of the pyrrole resonances (β_3) reflects fast exchange between three forms in equilibrium, i.e. Ni^{II}(STPP)Cl, [Ni^{II}(STPP)(1-MeIm)]Cl, and [Ni^{II}(STPP)(1-MeIm)$_2$]Cl. The chemical shift measured for the 1:1 molar ratio is very close to that established for the imidazole monoadduct (Table II). In this concentration range, [Ni^{II}(STPP)(1-MeIm)]Cl dominates the solution. The smooth change of the chemical shifts during the reaction allows the resonance assignments for both [Ni^{II}(STPP)(1-MeIm)]Cl and [Ni^{II}(STPP)(1-MeIm)$_2$]Cl on the basis of the correlation with the resonances of Ni^{II}(STPP)Cl (Table III). The titration of Ni^{II}(STPP)Cl with a primary amine, i.e. *N*-butylamine, is very similar to that described for the Ni^{II}(STPP)Cl–1-MeIm system. The smooth change of chemical shifts in the course of titration reflects the formation of mono and bis adducts that are undergoing fast exchange. The shift pattern of the thiaporphyrin resonances resembles that of imidazole systems.

Spectral Assignment for the Perchlorate Complex. Addition of $AgClO_4$ to the solution of Ni^{II}(STPP)Cl results in formation of the perchlorate complex Ni^{II}(STPP)ClO_4. The reaction has been followed by means of ^{1}H NMR spectroscopy, magnetic moment measurements in solution, and electronic spectroscopy. Addition of an excess of tetrabutylammonium perchlorate to a chloroform solution of Ni^{II}(STPP)Cl also yields Ni^{II}(STPP)ClO_4. The electronic spectra of the products are identical for both routes. A titration of Ni^{II}(STPP)Cl with $AgClO_4$·3CH_3CN in benzene or chloroform produced smooth changes in the chemical shift. Pyrrole and thiophene resonances exhibit dynamic line broadening due to the exchange between chloride and perchlorate anion:

$$Ni^{II}(STPP)Cl + Ni^{II}(STPP)^{*}ClO_4 \rightleftharpoons Ni^{II}(STPP)ClO_4 + Ni^{II}(STPP)^{*}Cl$$

The final spectra of the titration products are distinctly different for chloroform and benzene solutions. Ni^{II}(STPP)ClO_4 in benzene

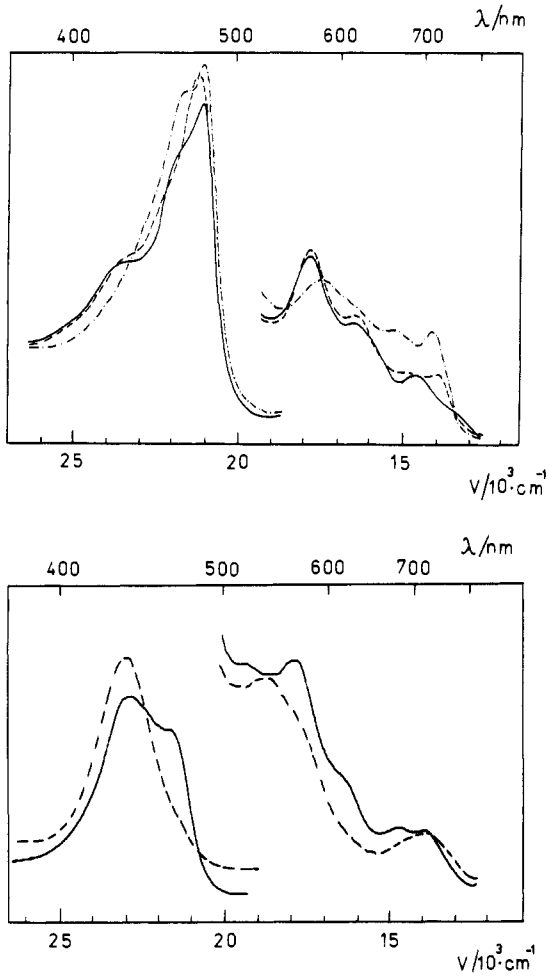

Figure 8. Electronic spectra. (Trace A, top): (—) Ni^{II}(STPP)Cl in chloroform; (---) Ni^{II}(STPP)Cl after addition of 1 equiv of imidazole: (-·-) Ni^{II}(STPP)Cl after addition of 10 equiv of imidazole. (Trace B, bottom): (---) Ni^{II}(STPP)(ClO_4) in chloroform; (—) Ni^{II}(STPP)(ClO_4) in benzene.

exhibits the paramagnetically shifted spectrum (pyrrole resonances 22.09, 15.45, 15.23 ppm; 298 K). The pattern of resonances resembles that of Ni^{II}(STPP)Cl. The deviation from the Curie-law behavior in the variable-temperature ^1H NMR spectra is noted for pyrrole resonances which can be accounted for by an equilibrium between diamagnetic and paramagnetic Ni^{II}(STPP)ClO_4 forms.

The ^1H NMR spectrum of Ni^{II}(STPP)ClO_4 in chloroform exhibits features characteristic of a diamagnetic metallothiaporphyrin[10,23] or 21-thiaporphyrin[29] (thiophene 9.65 ppm; pyrrole β_3 9.15 ppm, $\beta_{1,2}$ 9.60 and 9.20 ppm). In particular, a well-resolved AB pattern of pyrrole β_1, β_2 resonances with a typical J_{AB} = 5 Hz coupling constant has been observed. The relatively large Δ_{AB} = 37.6 Hz and the residual dependence of the chemical shifts on the $AgClO_4 \cdot 3CH_3CN$ concentration even for the 1:10 molar ratio result from the small contribution of the paramagnetic form to the chemical shifts.

Magnetic susceptibility measurements[30] have been made for Ni^{II}(STPP)ClO_4 in benzene and chloroform using Evan's method. The lower value of the magnetic moment in benzene (2.85 μ_B) as compared to that of Ni^{II}(STPP)Cl (3.3 μ_B)[9] reflects the equilibrium between paramagnetic and diamagnetic forms of Ni^{II}(STPP)ClO_4.

Electronic Spectra. The electronic spectral changes that accompany modifications in the coordination sphere of Ni(II) are shown in Figure 8.

The spectral characteristics resemble those of regular metalloporphyrins. Thus the intense features at 400 nm correspond to the porphyrin Soret band, and weaker features in the visible region are related to the porphyrin Q bands. Due to the lower symmetry of thiaporphyrin, the low-energy portion is more complex than found for the corresponding nickel porphyrin. The electronic spectra demonstrate typical patterns which reflect clearly a coordination number of Ni(II), while the replacement of axial ligands produces only minor modifications.

Discussion

Electronic Structure. The five- and six-coordinate complexes of the general formula Ni^{II}(STPP)L (L = Cl^-, Br^-, I^-, (*R*)-Im, $NH_2C_4H_9$) or [Ni^{II}(STPP)L_2]Cl ((*R*)-Im, DMSO, methanol) exhibit the properties of high-spin Ni(II) complexes with the electronic structure $d^2_{xy}d^2_{xz}d^2_{yz}d^1_{x^2-y^2}d^1_{z^2}$.[20,21]

Replacement of chloride by perchlorate results in formation of low-spin diamagnetic complex Ni^{II}(STPP)ClO_4 in chloroform. Complete dissociation of perchlorate anion or lengthening of the apical ligand–nickel distance and the simultaneous movement of Ni(II) into the plane of the macrocycle should result in the low-spin state.[31] A thermal equilibrium between two spin isomers related to a dynamic in-plane out-of-plane motion of five-coordinate Ni^{II}(STPP)ClO_4 or an equilibrium between five-coordinate (paramagnetic) and four-coordinate (diamagnetic) species can be suggested to account for the intermediate values of isotropic shift and magnetic moments in benzene. Differences in ClO_4^- solvation, π–π solvent–porphyrin, π–d_{z^2} solvent–Ni(II) interactions can also play an important role, as proposed for Fe^{III}(TPP)-ClO_4.[32,33]

Contribution to Isotropic Shift. It is generally argued that dipolar contribution to isotropic shift is negligible for five- or six-coordinate Ni(II) compounds.[34] Sizable dipolar shifts can arise as a result of the anisotropy of the zero field splitting (ZFS). The dipolar shift arising from ZFS have a characteristic T^{-2} dependence for high-spin d^8 in contrast to T^{-1} dependence expected for contact shifts.[34,35] In Curie plots of the chemical shifts vs T^{-1} for Ni^{II}(STPP)Cl the intercept at infinite temperature is close to the positions of a diamagnetic reference (Figure 4).

The relatively small magnitudes of deviations demonstrate that the dipolar term contribution to isotropic shift is negligible.

Shift direction alternation of the phenyl protons in paramagnetic metallotetraphenylporphyrins is characteristic if the π-contact shift is dominant, with the proton and methyl protons exhibiting shifts of opposite sign for any position on the ring. On the other hand dominant dipolar shifts are characterized by the shifts where the sign and magnitude are determined by the magnetic susceptibility tensor symmetry and its orientation with respect to the molecule.[36,37] The alternation of the direction of phenyl shifts in Ni^{II}(STPP)Cl is compatibile with the dominant π-contact contribution. Analyses of the temperature dependence and of the phenyl isotropic shift are in accord with dominance of contact contribution at the pyrrole and thiophene positions. The dipolar mechanism in Ni^{II}(NCH_3TPP)Cl also contributed less than 10% to the pyrrole shifts.[21] Phenyl ring rotation allows π-spin density delocalization onto the rings by removing the orthogonality of the phenyl and porphyrin π-systems. The downfield shift of pyrrole resonances is indicative of σ-delocalization of spin density and is consistent with the ground state of Ni(II) which has two unpaired

(29) Lisowski, J.; Grzeszczuk, M.; Latos-Grażyński, L. *Inorg. Chim. Acta* **1989**, *161*, 153.
(30) Evans, D. F.; James, T. A. *J. Chem. Soc., Dalton Trans.* **1979**, 723.
(31) (a) Orioli, P. L.; Ghilardi, C. A. *J. Chem. Soc. A* **1970**, 1511. (b) Orioli, P. L. *Coord. Chem. Rev.* **1971**, *6*, 285.
(32) Goff, H. M.; Shimomura, E. *J. Am. Chem. Soc.* **1980**, *102*, 31.
(33) Reed, C. A.; Mashiko, T.; Bentley, S. P.; Kastner, M. E.; Scheidt, W. R.; Spartalian, K.; Lang, G. *J. Am. Chem. Soc.* **1979**, *101*, 2949.
(34) La Mar, G. N., Horrocks, W. D., Holm, R. H., Eds. In *NMR of Paramagnetic Molecules*; Academic Press: New York, 1974; Chapters 1 and 4.
(35) (a) Kurland, R. J.; Mc Garvey, B. R. *J. Magn. Reson.* **1970**, *2*, 286. (b) Bleaney, B. J. *J. Magn. Reson.* **1972**, *8*, 91.
(36) Goff, H. M.; La Mar, G. N. *J. Am. Chem. Soc.* **1977**, *99*, 6599.
(37) Longueet-Higgins, H. C.; Rector, C. W.; Platt, J. R. *J. Chem. Phys.* **1950**, *18*, 1174.

electrons in the σ-symmetry orbitals ($d_{x^2-y^2}$, d_{z^2}).

A large difference in contact shifts of pyrrole resonances is seen even for protons located on the same pyrrole ring. The spread of shifts is related to the Ni(II) coordination number (Table I).

The upfield shift of the thiophene resonance requires special comment. The characteristic side-on coordination of the thiophene moiety changes the pathway of the spin delocalization. This folding of thiophene should reduce the σ-effect for the thiophene hydrogens, since the mechanism is strongly dependent on geometry.[19b] The unpaired spin density is localized on the sulfur σ-orbital that is not orthogonal to the π-orbitals of the thiaporphyrin, and σ–π overlap within the thiophene ring will permit the direct transfer of unpaired spin density from the sulfur σ pair into the π system without any π ligand–Ni(II) bonding. The spread of pyrrole resonances results from delocalization of positive π spin density (upfield shift). The mechanism resembles one proposed for $Ni^{II}(NCH_3TPP)Cl$ where the spin density from the methylated nitrogen produced an upfield shift of N-methylated pyrrole and differentation of downfield-shifted pyrroles.

Analysis of π Delocalization Mechanisms. Usually the π delocalization of unpaired spin density in metalloporphyrins is described in terms ligand-to-metal and metal-to-ligand charge transfer.[19] Spin densities at the particular carbons are related to the pattern of the Hückel occupied $3e_\pi$ and unoccupied $4e_\pi^*$ molecular orbitals.[37] This approach, formally valid for the D_{4h} symmetry, was applied with qualitative success to a large variety of metalloporphyrins of lower symmetry that was induced by five-coordination, asymmetry of natural porphyrins,[19] coordination of planar axial ligand(s),[38] and intrinsic asymmetry of meso-substituted porphyrins,[39] N-substituted porphyrins,[4c,40] and chlorins.[41] The replacement of the nitrogen by sulfur should have profound effect on the structure of the molecular orbitals involved in the spin density transfer. To account for the sulfur contribution and the geometry of 21-thiaporphyrin, the semiquantitative Fenske–Hall LCAO MO method has been used.[42] The idealized geometry of thiaporphyrin (bond lengths derived from the crystal structure[8]) has been used in the calculations. The thiophene ring has been arbitrarily located in the bent configuration (N_3 plane–thiophene dihedral angle 30°). The spin density transfer into or from thiaporphyrin π orbitals requires the direct involvement of the $d_{x^2-y^2}$ orbital of Ni^{II} and orbitals of sulfur included in the extensive conjugation of the folded thiaporphyrin. The extent of mixing of the thiaporphyrin molecular orbital with $d_{x^2-y^2}$ of nickel has been ascertained by considering first the symmetry and then the overlap between the Ni^{II} and thiaporphyrin orbitals. The energy separation relative to other accessible ligand π-orbitals has also been analyzed. The occupied molecular orbitals and the lowest unoccupied orbitals are presented in Figure 9. The ^1H NMR spectra of $[Ni^{II}(STPP)X]$ and $[Ni^{II}(STPP)X_2]$ can be qualitatively accounted for by considering four orbitals, ψ_{-6}, ψ_{-7}, ψ_{-9}, ψ_{-11}.

Delocalization of the unpaired spin density within the ψ_{-6} orbital determines the differentation of spin densities at the β_1 and β_2 carbons. The π spin density at the β_1 position is *lower* than at β_2, as expected on the basis of the NMR analysis. The observed contribution to the contact shift follows the same order (Tables I and II). The spin density at the β_3 position is determined mainly within the ψ_{-9} orbital. The relative contribution of this pathway should change from $[Ni^{II}(STPP)X]$ to $[Ni^{II}(STPP)X_2]$, as reflected in the NMR spectra.

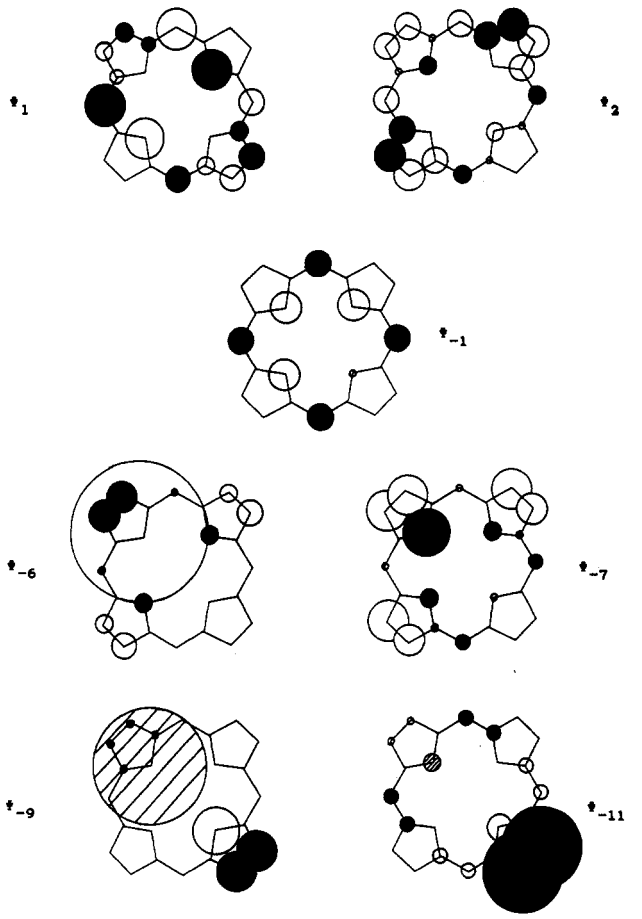

Figure 9. Unpaired spin density of occupied molecular π orbitals of 21-thiaporphyrin with appropriate symmetry, energy, and overlap to interact with the $d_{x^2-y^2}$ orbital of Ni^{II}. The LUMO's are also shown. Phases are indicated by unshaded and filled circles, with the size of the circle indicating relative spin densities. The contribution of all p_y orbitals of the sulfur hybrid is also presented (cross-hatched circle, y axis directed toward the macrocycle center). The orbital numbering is chosen with respect to the HOMO (ψ_{-1}) according to decreasing energy. The thiophene ring is located in the upper-left corner of the macrocycle.

The geometry of the five-coordinate $Ni^{II}(STPP)Cl$ has been described in the Introduction. The geometry of the six-coordinate forms should be similar to that of $Rh^{III}(STPP)Cl_2$.[10] The difference in the position of the Ni(II) ion in the five- and six-coordinate complexes is reflected in the amount of spin density delocalized to the pyrrole trans to the thiophene. This contribution is smaller for six-coordinate species so the respective resonance is shifted ca. 25 ppm downfield as compared to the five-coordinate one. A subtle modification of the $d_{x^2-y^2}$–ψ_{-9} overlap may produce this shift change.

The π spin density at the meso position and at the phenyl rings may result from the delocalization within each occupied orbital. Additionally, the fully occupied d_{xz} and d_{yz} orbitals can be engaged in extensive π-back-bonding into ψ^*_1 and ψ^*_2 orbitals. The net spin density in the d_π orbitals is polarized by the unpaired electrons in the $d_{x^2-y^2}$ and d_{z^2} orbitals via spin–orbit coupling. This mechanism can distribute π spin density to the meso carbons and the phenyl rings as discussed earlier for Ni(TPP)(pyridine) and $Ni^{II}(NCH_3TPP)Cl$.[20,21]

Imidazole Adducts. The strong similarities in pyrrole, thiophene, and phenyl paramagnetic shift patterns in the halide and mono (*R*)-imidazole complexes allow us to conclude that the shift origins are predominantly contact in both cases. The shifts for the various imidazole protons as listed in Table II are downfield for the NH, 2-H, 4-H, and 5-H protons, strongly upfield for 2-CH_3, and slightly

(38) (a) Walker, F. A.; Buehler, J.; West, J. T.; Hinds, J. L. *J. Am. Chem. Soc.* **1983**, *105*, 6923. (b) Traylor, T. G.; Berzinis, A. P. *J. Am. Chem. Soc.* **1980**, *102*, 2844. (c) Goff, H. *J. Am. Chem. Soc.* **1980**, *102*, 3252. (d) Momenteau, M.; Mispelter, J.; Loock, B.; Lhoste, J.-M. *J. Chem. Soc., Perkin. Trans. 1* **1985**, 221.

(39) Walker, F. A.; Balke, V. L.; McDermont, G. A. *J. Am. Chem. Soc.* **1982**, *104*, 1569.

(40) Balch, A. L.; Chan, Y.-W.; La Mar, G. N.; Renner, M. W. *Inorg. Chem.* **1985**, *24*, 1437.

(41) (a) Hanson, L. K.; Chang, C. K.; Davis, M. S.; Fajer, J. *J. Am. Chem. Soc.* **1981**, *103*, 663. (b) Pawlik, M. J.; Miller, P. K.; Sullivan, E. P., Jr.; Levstik, M. A.; Almond, D. A.; Strauss, S. H. *J. Am. Chem. Soc.* **1988**, *110*, 3007. (c) Chatfield, M. J.; La Mar, G. N.; Parker, W. D., Jr.; Smith, K. M.; Leung, H.-K.; Morris, I. K. *J. Am. Chem. Soc.* **1988**, *110*, 6352. (d) Liccocia, S.; Chatfield, M. J.; La Mar, G. N.; Smith, K. M.; Mansfield, K. E.; Anderson, R. R. *J. Am. Chem. Soc.* **1989**, *111*, 6087.

(42) Hall, M. B.; Fenske, R. F. *Inorg. Chem.* **1972**, *11*, 768.

upfield for 5-CH_3. This pattern is generally consistent with major contribution from σ-spin delocalization.[43] The sign change observed for 2-CH_3 and 2-H resonances suggests some contribution from a π delocalization mechanism.[44] In imidazole coordination to iron, including iron porphyrins, the upfield (downfield) shift of 2-H and downfield (upfield) shift of 2-CH_3 are considered as evidence for the π-delocalization mechanism.[44-46] The isotropic shift patterns for the following systems $[Ni^{II}(Im)_6]$,[43] $[Ni^{II}(acac)(1\text{-MeIm})]_2$,[47] $Ni^{II}(dpm)(1\text{-MeIm})_2$,[48] and $Ni^{II}(smdpt)(1\text{-MeIm})$[49] (acac = acetylacetonato, dpm = dipivaloylmethanato, smpdt = bis(γ-(salicylideneamino)propyl)-*N*-methylamine) are consistent with that presented here for $[Ni^{II}(STPP)((R)\text{-Im})]Cl$.

Conclusions

It is apparent from the ^1H NMR studies of $Ni^{II}(STPP)Cl$ and related systems that the 21-thiaporphyrin macrocycle is flexible in solution. The structure of the equatorial macrocycle adjusts to the spin and electronic state of $Ni^{II}(STPP)Cl$, as determined by the nature and number of axial ligands. The most profound effects of this property are the formation of low-spin $Ni^{II}(STPP)ClO_4$ and $Ni^{I}(STPP)$.[11] Thus a large range of ionic radii are accepted by the thiaporphyrin, and the binding cavity of thiaporphyrin changes due to rearrangement of the thiophene moiety. The ^1H NMR spectra of $Ni^{II}(STPP)Cl$ and $Ni^{II}(NCH_3TPP)Cl$[21] exhibit similarities that are related to the folding of macrocycles that is imposed by the coordination geometry of the donor centers. Current interest in the chemistry and spectroscopy of nickel porphyrins and related systems[50] is relevant to understanding cofactor F_{430}[12-17] properties, since this can coordinate axial ligands, change spin states, and be readily reduced to the Ni(I) form.[50-53]

Quite unexpectedly, some of these properties are mimicked by the chemistry of $Ni^{II}(STPP)Cl$. The hyperfine shift pattern for the imidazole ligands presents useful and potentially unique probes for detecting histydyl ligand coordination to the Ni(II) macrocycle including F_{430}.

Experimental Section

Solvents and Reagents. Chloroform-d_1 (IBJ), benzene-d_6 (IBJ), toluene-d_8 (Isotopes), and dimethyl-d_6 sulfoxide (IBJ) were dried over molecular sieves. Methanol-d_4 (IBJ) was used as received.

Substituted imidazoles (all from Aldrich), imidazole (Im), 4-methylimidazole (4(5)-MeIm), and 2-methylimidazole (2-MeIm), were purified by standard procedures. Imidazole-*2-d* and imidazole-d_4 were prepared according to reported methods.[54] Usually, imidazole-d_4 was used instead of imidazole-d_3 since the ND is easily replaced by the residual water in solution to form NH.

Silver perchlorate was recrystallized from acetonitrile to form $AgClO_4 \cdot 3CH_3CN$ and dried in small portions directly before use.

Preparation of Compounds. Tetraphenyl-21-thiaporphyrin derivatives ST(R)PPH were synthesized as described recently.[18] Selectively deuterated 5,20-diphenyl-10,15-bis(phenyl-d_5)-21-thiaporphyrin (STPPH-d_{10}) was synthesized in the same manner as STPPH using benzaldehyde-d_5 which was synthesized by oxidation of toluene-d_8 with $Ce(SO_4)_2$.[55]

STPPH-d_6 (deuterated at the pyrrole β-positions) was prepared from pyrrole-d_5.[8,29,56]

Ni(II) complexes were prepared as described recently.[9]

Instrumentation. ^1H NMR spectra were measured on Tesla 80, Tesla 100, and QE 300 spectrometers operating in the quadrature detection mode (^1H frequencies are 80, 100, and 300 MHz, respectively). A total of 1000 scans were taken. The signal to noise ratio was improved by appodization of the free induction decay which induced typically 5–15-Hz broadening. The peaks were referenced against tetramethylsilane. Proton NOE measurements were performed on Tesla 80 and Tesla 100 spectrometers. Data points (16K) were collected over the 15-kHz bandwidth. The nuclear Overhauser effects were recorded by application of a presaturation pulse of 1 s with the decoupler on-resonance. Corresponding reference spectra were collected under identical conditions but with the decoupler off-resonance. Difference spectra were obtained by subtracting the transformed off-resonance spectrum from the on-resonance spectrum. Typical NOE spectra consisted of at least 1000 transients. Magnetic moment measurements were carried out by Evan's method with $CDCl_3$ or C_6D_6 solutions using TMS as reference.[33] Diamagnetic corrections were obtained using the published values of the constitutive corrections for $TPPH_2$[57] and Pascal's constants.

Electronic spectra were measured with a Specord UV–vis spectrophotometer.

Registry No. Ni(STPP)Cl, 119145-09-4; Ni(STPP-d_6)Cl, 139944-16-4; Ni(STPP-d_{10})Cl, 139944-17-5; Ni(STPP)Br, 139944-18-6; Ni(STPP)I, 139944-19-7; [Ni(STPP)(Im)]Cl, 139944-20-0; [Ni(STPP)(2-MeIm)]Cl, 139944-21-1; [Ni(STPP)(5-MeIm)]Cl, 139944-22-2; [Ni(STPP)(1-MeIm)]Cl, 139944-23-3; $[Ni(STPP)(Im)_2]Cl$, 139944-24-4; $[Ni(STPP)(1\text{-MeIm})_2]Cl$, 139944-25-5.

(43) Wicholas, M.; Mustatich, R.; Johnson, B.; Smedley, T.; May, J. *J. Am. Chem. Soc.* **1975**, *97*, 2113.
(44) Balch, A. L.; Chan, Y.-W.; La Mar, G. N.; Latos-Grażyński, L.; Renner, M. W. *Inorg. Chem.* **1985**, *24*, 1437.
(45) Satterlee, J. D.; La Mar, G. N. *J. Am. Chem. Soc.* **1976**, *98*, 2804.
(46) Wu, F.-J.; Kurtz, D. M., Jr. *J. Am. Chem. Soc.* **1989**, *111*, 6563.
(47) Tovrog, B. S.; Drago, R. S. *J. Am. Chem. Soc.* **1974**, *96*, 2804.
(48) Claramunt, R.-M.; Elquero, J.; Jacquier, R. *Org. Magn. Reson.* **1971**, *3*, 595.
(49) Tovrog, B. S.; Drago, R. S. *J. Am. Chem. Soc.* **1977**, *99*, 2203.
(50) Shiemke, A. K.; Kaplan, W. A.; Hamilton, C. L.; Shelnutt, J. A. Scott, R. A. *J. Biol. Chem.* **1989**, *264*, 7276.
(51) Shelnutt, J. A.; Ho, J.-Y.; Yu, N.-T.; Yamamoto, T.; Rifkind, J. M. *Biochemistry* **1986**, *25*, 620.
(52) Eidsness, M. K.; Sullivan, R. J.; Schwartz, J. R.; Hartzel, P.; Wolfe, R. S.; Flank, A.-M.; Cramer, S. P.; Scott, R. A. *J. Am. Chem. Soc.* **1986**, *108*, 3120.
(53) Shiemke, A. K.; Scott, R. A.; Shelnutt, J. A. *J. Am. Chem. Soc.* **1988**, *110*, 1645.
(54) Vaugh, J. D.; Mugharbi, Z.; Wu, E. C. *J. Org. Chem.* **1970**, *31*, 1141.
(55) Syper, L. *Tetrahedron Lett.* **1966**, 4493.
(56) Boersma, A. D.; Goff, H. M. *Inorg. Chem.* **1982**, *21*, 581.
(57) Eaton, S. S.; Eaton, G. A. *Inorg. Chem.* **1980**, *19*, 1095.